



Polarization-resolved scintillations in Young's experiment

YARU GAO,^{1,2,7} YANGJIAN CAI,^{1,2,3,8} ARI T. FRIBERG,⁴ AND TACO D. VISSER^{1,5,6,9} 

¹Shandong Provincial Engineering and Technical Center of Light Manipulations and Shandong Provincial Key Laboratory of Optics and Photonic Devices, School of Physics and Electronics, Shandong Normal University, Jinan, 250014, China

²Collaborative Innovation Center of Light Manipulations and Applications, Shandong Normal University, Jinan, 250358, China

³School of Physical Science and Technology, Soochow University, Suzhou, 215006, China

⁴Institute of Photonics, University of Eastern Finland, Joensuu, FI-80101, Finland

⁵The Institute of Optics, University of Rochester, Rochester, New York, 14627, USA

⁶Department of Physics and Astronomy, Vrije Universiteit, Amsterdam, 1013LP, The Netherlands

⁷gaoyaru@sdu.edu.cn

⁸yangjiancai@suda.edu.cn

⁹tvisser@nat.vu.nl

Abstract: The conventional scintillation, or intensity fluctuation, that occurs in random electromagnetic beams is just one member of a broader class of four interconnected, polarization-resolved scintillations. We examine these generalized scintillations, called *Stokes scintillations*, that occur when two stochastic electromagnetic beams are made to interfere in Young's experiment. We find that the magnitude of the conventional scintillation can be decreased, within certain limits, at the expense of an increase of one or more of the other Stokes scintillations. For certain applications however, it may be beneficial to suppress the latter.

© 2022 Optica Publishing Group under the terms of the [Optica Open Access Publishing Agreement](#)

1. Introduction

Every random field displays intensity fluctuations or scintillations. Especially for the case of laser beams that propagate through atmospheric turbulence these have been studied extensively [1, Ch. 8]. However, even on free-space propagation an optical field can exhibit scintillation when it is generated by a partially coherent source [2]. Scintillations are of obvious concern in optical communications because they are a source of signal degradation, quantified by the scintillation index. Understanding how scintillation arises and how it may be controlled is both of fundamental and of practical importance.

The superposition of two scalar waves in Young's experiment shows a direct relation between their spatial coherence and the visibility of the ensuing intensity fringes [3]. Electromagnetic two-beam interference is more complex and cannot be described just in terms of intensity fringes. For example, the combination of two beams with orthogonal linear polarization and a fixed phase difference does not produce a modulation of intensity. However, it does lead to a polarization modulation because the superposition is elliptically polarized. An analysis of the changes in the polarization state and the degree of polarization in Young's experiment was reported in [4–6]. Further studies of the effect on the Stokes parameters caused by beam superposition are found in [7–10]. In the context of quantum optics, polarization modulation has been examined in [11,12]. The evolution of the Stokes parameters in partially coherent Gaussian Schell-model beams has been investigated in several studies, for example [13–15].

The four spectral Stokes parameters at position \mathbf{r} at frequency ω and their fluctuations are denoted $S_j(\mathbf{r}, \omega)$ and $\Delta S_j(\mathbf{r}, \omega)$, respectively, with $j \in \{1, 2, 3, 4\}$. In [16] a generalization of the

Hanbury Brown-Twiss (HBT) effect [17], namely the expectation value $\langle \Delta S_i(\mathbf{r}_1, \omega) \Delta S_j(\mathbf{r}_2, \omega) \rangle$ was introduced. The conventional HBT effect is described by $\langle \Delta S_0(\mathbf{r}_1, \omega) \Delta S_0(\mathbf{r}_2, \omega) \rangle$, which is therefore one of sixteen possible correlations of Stokes fluctuations. Setting the two observations points equal then leads to the notion of *Stokes scintillations* $\langle [\Delta S_j(\mathbf{r}, \omega)]^2 \rangle$. Since the first Stokes parameter represents the total spectral density (the intensity at frequency ω) of an electromagnetic beam, the variance of $S_0(\mathbf{r}, \omega)$ is identical with its scintillation. Clearly then, the conventional scintillation is just one of four different Stokes scintillations. Remarkably, these polarization-resolved scintillations are not independent but were shown, under the assumption of Gaussian statistics, to obey a sum rule. That means that an increase (decrease) of the traditional scintillation is accompanied by a decrease (increase) of one or more of the other three Stokes scintillations at the same point. This explains the observation, made several years ago, that scintillation and polarization fluctuations occur simultaneously [18]. In [19] the generalized HBT effect and the Stokes scintillations were examined in the far zone of Gaussian Schell-model sources. It was found that the different correlations and scintillations have varying spatial distributions, and that their dependence on the source parameters differs significantly. For the case of a random electromagnetic beam that is focused by a thin paraxial lens [20], the distribution of the Stokes scintillations across the focal plane has a complicated structure. Moreover, the generalized Hanbury Brown–Twiss correlations are strongly influenced by the focusing process. Their maximum value can be either lower or higher than that of the same correlation in the front focal plane.

In the present study the fundamental problem of the superposition of two random electromagnetic beams is analyzed. In particular, we examine the four Stokes scintillations in the context of Young's interference experiment. We study, for the case of far-zone points on the central axis, how their magnitudes depend on the spatial correlation of the two beams. We show that a trade-off between the relative strength of these generalized scintillations is possible. This means that the classical scintillation can be reduced, but inevitably at the expense of an increase of the fluctuations of the polarization states described by the Stokes parameters S_1 , S_2 or S_3 . As we will discuss, for certain applications it may be desirable to suppress not S_0 , but rather one of the other three scintillations. We begin, in Section 2., with a brief review of the polarization-resolved formalism that we employ. This section also introduces the notation that we use. This is followed by a description of two-beam interference in Section 3., for the case of an electromagnetic Gaussian Schell-model (GSM) source covered by a screen with two pinholes. From the analytic expression that are obtained for the four Stokes scintillations several conclusions are drawn, and possible applications are discussed.

2. Random beams and Stokes parameters

In the space-frequency domain, the state of coherence and polarization of a stochastic electromagnetic beam-like field that propagates along the z axis may be characterized by the cross-spectral density (CSD) matrix [3]

$$\mathbf{W}(\mathbf{r}_1, \mathbf{r}_2, \omega) = \begin{pmatrix} W_{xx} & W_{xy} \\ W_{yx} & W_{yy} \end{pmatrix}, \quad (1)$$

where all the matrix elements are functions of the same three variables and given by the expression

$$W_{ij}(\mathbf{r}_1, \mathbf{r}_2, \omega) = \langle E_i^*(\mathbf{r}_1, \omega) E_j(\mathbf{r}_2, \omega) \rangle, \quad (i, j = x, y). \quad (2)$$

Here $E_i(\mathbf{r}, \omega)$ denotes a Cartesian component of the electric field at position \mathbf{r} at frequency ω , and the angled brackets indicate an average taken over an ensemble of beam realizations. For brevity we will from now on no longer display the ω dependence.

The 2 by 2 identity matrix, denoted σ^0 , and the three Pauli spin matrices are defined as

$$\sigma^0 = \begin{pmatrix} 1 & 0 \\ 0 & 1 \end{pmatrix}, \quad \sigma^1 = \begin{pmatrix} 1 & 0 \\ 0 & -1 \end{pmatrix}, \quad \sigma^2 = \begin{pmatrix} 0 & 1 \\ 1 & 0 \end{pmatrix}, \quad \sigma^3 = \begin{pmatrix} 0 & -i \\ i & 0 \end{pmatrix}, \quad (3)$$

respectively. The Stokes parameters can be written as [21]

$$S_n(\mathbf{r}) = \mathbf{E}(\mathbf{r})^\dagger \sigma^n \mathbf{E}(\mathbf{r}), \quad (4)$$

where \dagger denotes the Hermitian conjugate and

$$\mathbf{E}(\mathbf{r}) = \begin{pmatrix} E_x(\mathbf{r}) \\ E_y(\mathbf{r}) \end{pmatrix}. \quad (5)$$

Hence their expectation values are

$$\langle S_n(\mathbf{r}) \rangle = \sum_{a,b} \sigma_{ab}^n W_{ab}(\mathbf{r}, \mathbf{r}), \quad (a, b = x, y). \quad (6)$$

More explicitly,

$$\langle S_0(\mathbf{r}) \rangle = W_{xx}(\mathbf{r}, \mathbf{r}) + W_{yy}(\mathbf{r}, \mathbf{r}), \quad (7)$$

$$\langle S_1(\mathbf{r}) \rangle = W_{xx}(\mathbf{r}, \mathbf{r}) - W_{yy}(\mathbf{r}, \mathbf{r}), \quad (8)$$

$$\langle S_2(\mathbf{r}) \rangle = W_{xy}(\mathbf{r}, \mathbf{r}) + W_{yx}(\mathbf{r}, \mathbf{r}), \quad (9)$$

$$\langle S_3(\mathbf{r}) \rangle = i[W_{yx}(\mathbf{r}, \mathbf{r}) - W_{xy}(\mathbf{r}, \mathbf{r})]. \quad (10)$$

In the case of a stochastic beam, the Stokes parameters are random quantities. The fluctuations around their average value are

$$\Delta S_n(\mathbf{r}) \equiv S_n(\mathbf{r}) - \langle S_n(\mathbf{r}) \rangle, \quad (n = 0, 1, 2, 3), \quad (11)$$

where $S_n(\mathbf{r})$ is the Stokes parameter of a single realization. As mentioned above, the concept of scintillation, measured as the variance of the spectral density at a point of observation, can be generalized to the fluctuation of all four spectral Stokes parameters [16]. These are defined as

$$D_n(\mathbf{r}) \equiv \langle [\Delta S_n(\mathbf{r})]^2 \rangle. \quad (12)$$

Because $S_0(\mathbf{r}, \omega)$ represents the total spectral density, it follows that $D_0(\mathbf{r})$ is equivalent to the traditional expression for the scintillation [1, Ch. 8]. The $D_n(\mathbf{r})$ coefficients are described by fourth-order statistical quantities. Under the assumption of Gaussian statistics one can employ the Gaussian moment theorem [17, Sec. 1.6.1] to write them in terms of second-order correlations

given by the CSD matrix (see Appendix A):

$$D_0(\mathbf{r}) = [W_{xx}(\mathbf{r}, \mathbf{r})]^2 + 2|W_{xy}(\mathbf{r}, \mathbf{r})|^2 + [W_{yy}(\mathbf{r}, \mathbf{r})]^2, \quad (13)$$

$$D_1(\mathbf{r}) = [W_{xx}(\mathbf{r}, \mathbf{r})]^2 - 2|W_{xy}(\mathbf{r}, \mathbf{r})|^2 + [W_{yy}(\mathbf{r}, \mathbf{r})]^2, \quad (14)$$

$$D_2(\mathbf{r}) = 2 [W_{xx}(\mathbf{r}, \mathbf{r})W_{yy}(\mathbf{r}, \mathbf{r}) + \text{Re}\{[W_{xy}(\mathbf{r}, \mathbf{r})]^2\}], \quad (15)$$

$$D_3(\mathbf{r}) = 2 [W_{xx}(\mathbf{r}, \mathbf{r})W_{yy}(\mathbf{r}, \mathbf{r}) - \text{Re}\{[W_{xy}(\mathbf{r}, \mathbf{r})]^2\}]. \quad (16)$$

It is easily verified that

$$\sum_{n=0}^3 D_n(\mathbf{r}) = 2 [W_{xx}(\mathbf{r}, \mathbf{r}) + W_{yy}(\mathbf{r}, \mathbf{r})]^2. \quad (17)$$

A normalized version of these four quantities is

$$d_n(\mathbf{r}) \equiv \frac{\langle [\Delta S_n(\mathbf{r})]^2 \rangle}{\langle S_0(\mathbf{r}) \rangle^2}. \quad (18)$$

It immediately follows from Eqs. (7) and (17) that the four Stokes scintillations are not independent but satisfy the sum rule

$$\sum_{n=0}^3 d_n(\mathbf{r}) = 2. \quad (19)$$

This expression shows that, at least in principle, one can tailor a beam such that one particular Stokes scintillation is optimized, albeit at the expense of the others. We note that $d_0(\mathbf{r})$ is the square of the scintillation index [1]. It is bounded by the inequalities [2]

$$1/2 \leq d_0(\mathbf{r}) \leq 1. \quad (20)$$

From the definitions (13)–(16) and (18) it follows that

$$0 \leq d_p(\mathbf{r}) \leq 1, \quad (p = 1, 2, 3). \quad (21)$$

3. Two-beam interference

Let us examine the behavior of the Stokes scintillations that are produced in Young's experiment, as sketched in Fig. 1. We take the observation point P to be far away from the two apertures and close to the z axis, i.e., in the paraxial region. In that case the field at P has a negligible longitudinal component and is of the form

$$\mathbf{E}(P) = K_1 \mathbf{E}(\mathbf{r}_1) + K_2 \mathbf{E}(\mathbf{r}_2), \quad (22)$$

with the propagators

$$K_m = -\frac{idS}{\lambda} \frac{e^{ikR_m}}{R_m}, \quad (m = 1, 2), \quad (23)$$

where dS denotes the area of the two pinholes, λ and k are the free-space wavelength and the wavenumber corresponding to frequency ω , and the distance $R_m = |\mathbf{r}_m P|$ [22, Sec. 8.2]. From Eq. (22) it is found that

$$\begin{aligned} W_{ij}(P, P) &= |K_1|^2 W_{ij}^{(0)}(\mathbf{r}_1, \mathbf{r}_1) + K_1^* K_2 W_{ij}^{(0)}(\mathbf{r}_1, \mathbf{r}_2) \\ &\quad + K_2^* K_1 W_{ij}^{(0)}(\mathbf{r}_2, \mathbf{r}_1) + |K_2|^2 W_{ij}^{(0)}(\mathbf{r}_2, \mathbf{r}_2), \end{aligned} \quad (24)$$

where $\mathbf{W}^{(0)}$ denotes the CSD matrix at the two pinholes. Since $P = (x, 0, L)$ is in the far zone, and because of the assumption of paraxiality, $1/R_1 \approx 1/R_2 \approx 1/L$. Likewise, $R_2 - R_1 \approx 2xd/L$.

Hence

$$W_{ij}(P, P) = \left(\frac{dS}{\lambda L} \right)^2 \left[W_{ij}^{(0)}(\mathbf{r}_1, \mathbf{r}_1) + W_{ij}^{(0)}(\mathbf{r}_1, \mathbf{r}_2)e^{ik\Delta} + W_{ij}^{(0)}(\mathbf{r}_2, \mathbf{r}_1)e^{-ik\Delta} + W_{ij}^{(0)}(\mathbf{r}_2, \mathbf{r}_2) \right], \quad (25)$$

where $\Delta = 2xd/L$.

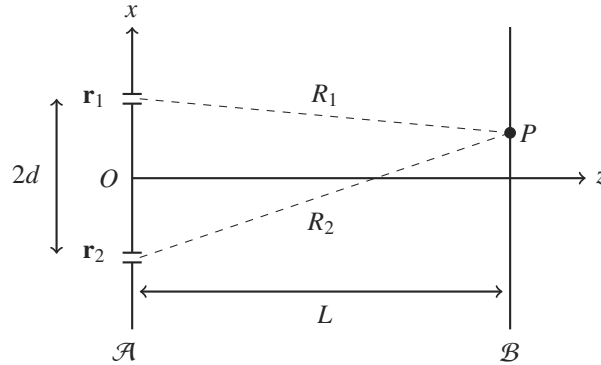


Fig. 1. The superposition of the fields radiated by two identical pinholes at $\mathbf{r}_1 = (d, 0, 0)$ and $\mathbf{r}_2 = (-d, 0, 0)$ in an opaque screen \mathcal{A} is observed at $P = (x, 0, L)$ on a parallel screen \mathcal{B} . The origin O is located midway between the apertures. The two distances are $R_1 = |\mathbf{r}_1 P|$, and $R_2 = |\mathbf{r}_2 P|$.

We illustrate the consequences of Eq. (25) by assuming the field at the pinholes to be that of a Gaussian Schell-model (GSM) source that is centered on the z axis [3]. When the effective width of both Cartesian field components is taken to be σ , then

$$W_{ij}^{(0)}(\boldsymbol{\rho}_1, \boldsymbol{\rho}_2) = A_i A_j B_{ij} e^{-(\rho_1^2 + \rho_2^2)/(4\sigma^2)} e^{-(\rho_2 - \rho_1)^2/(2\delta_{ij}^2)}. \quad (26)$$

Here $\boldsymbol{\rho} = (x, y)$ is a 2D vector in the plane $z = 0$, A_i is the amplitude of E_i , B_{ij} is the polarization correlation coefficient, and the δ_{ij} denote coherence radii. The parameters B_{ij} and δ_{ij} are independent of position, but may depend on frequency. The conditions they must satisfy are listed in Appendix B. A GSM source may be characterized by eight parameters [23]. In order to simplify the analysis, we introduce two assumptions. We take the spectral amplitudes to be equal ($A_x = A_y = A$), just as two of the coherence radii, i.e., $\delta_{xx} = \delta_{yy} = \delta$. In that case

$$W_{ij}^{(0)}(\mathbf{r}_n, \mathbf{r}_n) = A^2 B_{ij} e^{-d^2/(2\sigma^2)}, \quad (27)$$

$$W_{ij}^{(0)}(\mathbf{r}_1, \mathbf{r}_2) = A^2 B_{ij} e^{-d^2/(2\sigma^2)} e^{-2d^2/\delta_{ij}^2}, \quad (28)$$

from which it follows that at the observation point P

$$W_{ij}(P, P) = 2 \left(\frac{AdS}{\lambda L} \right)^2 e^{-d^2/(2\sigma^2)} B_{ij} \left[1 + e^{-2d^2/\delta_{ij}^2} \cos(k\Delta) \right]. \quad (29)$$

On substituting from Eq. (29) into the expressions (13)–(16) we obtain the Stokes scintillations at P . Restricting our attention to observation points on the central axis ($x = 0$), we find that

$$d_0(P) = \frac{1}{2} \left[1 + |B_{xy}|^2 \left(\frac{1 + e^{-2d^2/\delta_{xy}^2}}{1 + e^{-2d^2/\delta^2}} \right)^2 \right], \quad (30)$$

$$d_1(P) = \frac{1}{2} \left[1 - |B_{xy}|^2 \left(\frac{1 + e^{-2d^2/\delta_{xy}^2}}{1 + e^{-2d^2/\delta^2}} \right)^2 \right], \quad (31)$$

$$d_2(P) = \frac{1}{2} \left[1 + |B_{xy}|^2 \cos(2\phi) \left(\frac{1 + e^{-2d^2/\delta_{xy}^2}}{1 + e^{-2d^2/\delta^2}} \right)^2 \right], \quad (32)$$

$$d_3(P) = \frac{1}{2} \left[1 - |B_{xy}|^2 \cos(2\phi) \left(\frac{1 + e^{-2d^2/\delta_{xy}^2}}{1 + e^{-2d^2/\delta^2}} \right)^2 \right]. \quad (33)$$

Here ϕ denotes the phase of B_{xy} . It is readily verified that these four quantities satisfy the sum rule (19). We note that the far-zone, on-axis polarization-resolved scintillations depend on the scaled coherence radii δ/d , δ_{xy}/d , and the correlation coefficient B_{xy} . These three quantities are interrelated through the inequalities (see Appendix B)

$$\delta \leq \delta_{xy} \leq \frac{\delta}{\sqrt{|B_{xy}|}}, \quad (34)$$

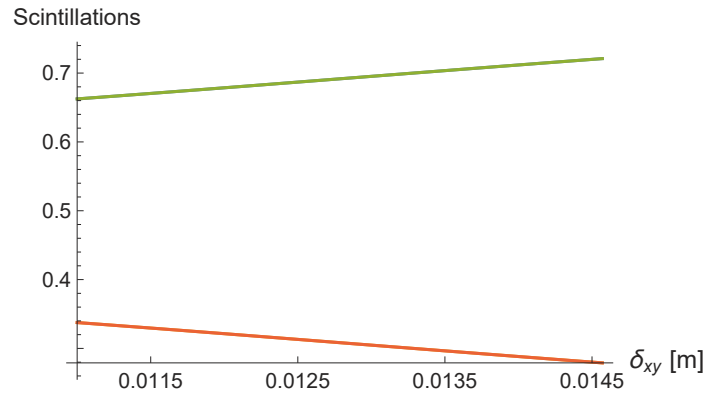


Fig. 2. The spectrally-resolved scintillations $d_0(P)$ (upper green curve) and $d_1(P)$ (lower red curve) when δ_{xy} is varied between its bounds given by Eq. (34). In this example $B_{xy} = 0.57$, $d = 1$ cm, and $\delta = 1.1$ cm.

From the expressions for the four Stokes scintillations we infer that

- The traditional scintillation, $d_0(P)$, reaches its minimum value of $1/2$ when the correlation coefficient $|B_{xy}| = 0$, i.e., when the field at both pinholes is unpolarized. In that case all four Stokes scintillations are $1/2$.
- For a non-zero B_{xy} coefficient the value of $d_0(P)$ attains its maximum when the coherence radius δ_{xy} equals its upper bound. The second Stokes scintillation, $d_1(P)$, then reaches its minimum. This behavior is illustrated in Fig. 2. We note that in this example δ_{xy} is varied over the entire range of possible values given by the bounds (34).
- The extrema of the first two scintillations coincide with those of $d_2(P)$ and $d_3(P)$.
- The presence of the cosine term in Eqs. (32) and (33) means that unless B_{xy} is real-valued ($\phi = 0$ or π), the modulations of $d_2(P)$ and $d_3(P)$ will be less than those of the other two scintillations.

- For fields with a high spatial correlation, i.e., both δ/d and δ_{xy}/d much larger than one, the factor in round brackets in Eqs. (30)–(33) reduces to unity. The four scintillations are then solely governed by the correlation coefficient B_{xy} . An example is shown in Fig. 3. It is seen, at least in this specific example, that d_0 and d_2 are correlated, and anti-correlated with d_1 and d_3 .
- On making use of Eq. (27) it follows that at the two pinholes

$$d_0(\mathbf{r}_m) = \frac{1}{2} \left(1 + |B_{xy}|^2 \right), \quad (m = 1, 2). \quad (35)$$

We can compare this with Eq. (30). Because, according to Eq. (34), $\delta_{xy} \geq \delta$, it is seen that the traditional scintillation of the superposed fields at P is greater than or equal to the scintillation of the individual fields at the two pinholes:

$$d_0(P) \geq d_0(\mathbf{r}_m), \quad (m = 1, 2). \quad (36)$$

The sum rule (19) allows the suppression of one type of scintillation at the expense of an increase of the other scintillations. For example, minimizing the traditional scintillation d_0 by reducing $|B_{xy}|$ (as in Fig. 3) may be used to suppress unwanted speckle. However, one can also envision applications, see [24] and the references therein, where a field interacts with a chiral structure. In that case, optimizing the stability of S_3 by minimizing d_3 may be preferable. This can be achieved by increasing $|B_{xy}|$. Similarly, when the two combined fields are made to pass through a birefringent medium as, for example, certain types of optical fibers [25], it may be useful to stabilize the linear polarization by reducing d_1 .

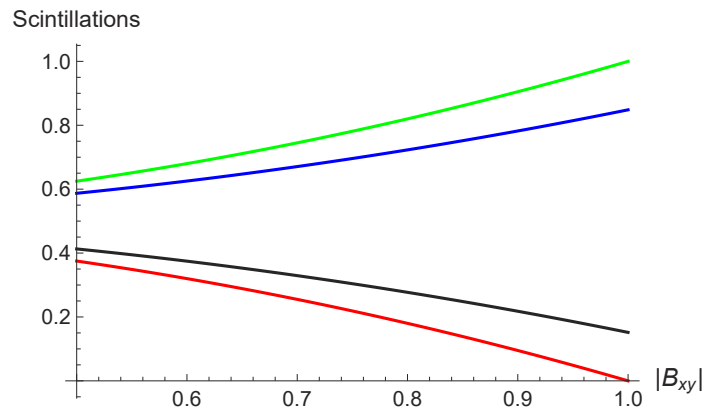


Fig. 3. The four polarization-resolved scintillations as a function of the modulus of the polarization correlation coefficient B_{xy} . From top to bottom: $d_0(P)$ (green), $d_2(P)$ (blue), $d_3(P)$ (black), and $d_1(P)$ (red). In this example $\phi = 0.4$, $d = 1$ cm, and $\delta = \delta_{xy} = 2$ cm.

It is worth noting that the different Stokes scintillations can be measured using a narrow-band spectral filter together with a division-of-amplitude photopolarimeter (see, for example, [26] and the references therein).

4. Conclusions

In summary, we have examined the paraxial far-zone, polarization-resolved scintillations that occur when random beams are combined in Young's interference experiment. The assumption of Gaussian statistics allows the derivation of expressions in terms of second-order correlation

quantities. As illustrated by two examples, the sum rule that relates the four spectral Stokes scintillations allows a trade-off between them. Depending on the application at hand, the stability of one particular Stokes parameter can be increased at the expense of an increase of the variance of one or more of the others.

Appendix A

From the definition (12) we have that

$$D_n(\mathbf{r}) = \langle [\Delta S_n(\mathbf{r})]^2 \rangle \tag{37}$$

$$= \langle S_n(\mathbf{r})S_n(\mathbf{r}) \rangle - \langle S_n(\mathbf{r}) \rangle^2. \tag{38}$$

The first term on the right-hand side is a fourth-order correlation. The assumption of Gaussian statistics allows us to use the Gaussian moment theorem [17, Sec. 1.6.1] to write this in terms of the CSD matrix, namely

$$\langle S_n(\mathbf{r})S_n(\mathbf{r}) \rangle = \sum_{a,b} \sum_{c,d} \sigma_{ab}^n \sigma_{cd}^n \langle E_a^*(\mathbf{r})E_b(\mathbf{r})E_c^*(\mathbf{r})E_d(\mathbf{r}) \rangle \tag{39}$$

$$= \sum_{a,b} \sum_{c,d} \sigma_{ab}^n \sigma_{cd}^n [\langle E_a^*(\mathbf{r})E_b(\mathbf{r}) \rangle \langle E_c^*(\mathbf{r})E_d(\mathbf{r}) \rangle + \langle E_a^*(\mathbf{r})E_d(\mathbf{r}) \rangle \langle E_c^*(\mathbf{r})E_b(\mathbf{r}) \rangle] \tag{40}$$

$$= \sum_{a,b} \sum_{c,d} \sigma_{ab}^n \sigma_{cd}^n [W_{ab}(\mathbf{r}, \mathbf{r})W_{cd}(\mathbf{r}, \mathbf{r}) + W_{ad}(\mathbf{r}, \mathbf{r})W_{cb}(\mathbf{r}, \mathbf{r})]. \tag{41}$$

Applying this for the case $n = 0$ while noticing that the quadruple summation yields only four non-zero terms, gives us

$$D_0(\mathbf{r}) = [W_{xx}(\mathbf{r}, \mathbf{r})]^2 + [W_{yy}(\mathbf{r}, \mathbf{r})]^2 + 2 |W_{xy}(\mathbf{r}, \mathbf{r})|^2, \tag{42}$$

which is Eq. (13). The derivation of the other three Stokes fluctuations is completely similar.

Appendix B

The source parameters cannot be chosen arbitrarily, but must satisfy certain constraints. Specifically, it follows from the definition of the CSD matrix that [3, Chap. 9]

$$B_{xx} = B_{yy} = 1, \tag{43}$$

$$B_{xy} = B_{yx}^*, \tag{44}$$

$$|B_{xy}| \leq 1, \tag{45}$$

$$\delta_{xy} = \delta_{yx}. \tag{46}$$

Realizability conditions have been derived in [27], namely

$$\sqrt{\frac{\delta_{xx}^2 + \delta_{yy}^2}{2}} \leq \delta_{xy} \leq \sqrt{\frac{\delta_{xx}\delta_{yy}}{|B_{xy}|}}, \tag{47}$$

and

$$|B_{xy}| \leq \frac{2}{\delta_{xx}/\delta_{yy} + \delta_{yy}/\delta_{xx}}. \tag{48}$$

For the case that we consider, $\delta_{xx} = \delta_{yy} = \delta$, the last two constraints reduce to

$$\delta \leq \delta_{xy} \leq \frac{\delta}{\sqrt{|B_{xy}|}}, \tag{49}$$

which is Eq. (34), and

$$|B_{xy}| \leq 1. \tag{50}$$

Funding. National Key Research and Development Program of China (2019YFA0705000); National Natural Science Foundation of China (11904211, 11974218, 12192254, 91750201, 11525418); Innovation Group of Jinan (2018GXRC010); Local Science and Technology Development Project of the Central Government (YDZX20203700001766); Dutch Research Council (P19-13 Optical wireless super highways); Joensuu University Foundation; Academy of Finland (310511, 320166); .

Disclosures. The authors declare no conflicts of interest.

Data availability. Data underlying the results presented in this paper are not publicly available at this time but may be obtained from the authors upon reasonable request.

References

1. L. C. Andrews and R. L. Phillips, *Laser Beam Propagation through Random Media*, 2nd ed. (SPIE, 2005).
2. A. T. Friberg and T. D. Visser, "Scintillation of electromagnetic beams generated by quasi-homogeneous sources," *Opt. Commun.* **335**, 82–85 (2015).
3. E. Wolf, *Introduction to the Theory of Coherence and Polarization of Light* (Cambridge University Press, 2007).
4. F. Gori, M. Santarsiero, R. Borghi, and E. Wolf, "Effects of coherence on the degree of polarization in a Young interference pattern," *Opt. Lett.* **31**(6), 688–690 (2006).
5. T. Setälä, J. Tervo, and A. T. Friberg, "Stokes parameters and polarization contrasts in Young's interference experiment," *Opt. Lett.* **31**(14), 2208–2210 (2006).
6. T. Setälä, J. Tervo, and A. T. Friberg, "Contrasts of Stokes parameters in Young's interference experiment and electromagnetic degree of coherence," *Opt. Lett.* **31**(18), 2669–2671 (2006).
7. T. D. Visser and R. W. Schoonover, "A cascade of singular field patterns in Young's interference experiment," *Opt. Commun.* **281**(1), 1–6 (2008).
8. A. T. Friberg and T. Setälä, "Electromagnetic theory of optical coherence," *J. Opt. Soc. Am. A* **33**(12), 2431–2442 (2016).
9. H. Partanen, B. J. Hoenders, A. T. Friberg, and T. Setälä, "Young's interference experiment with electromagnetic narrowband light," *J. Opt. Soc. Am. A* **35**(8), 1379–1384 (2018).
10. A. Hannonen, B. J. Hoenders, W. Elsässer, A. T. Friberg, and T. Setälä, "Ghost polarimetry using Stokes correlations," *J. Opt. Soc. Am. A* **37**(5), 714–719 (2020).
11. A. Norrman, K. Blomstedt, T. Setälä, and A. T. Friberg, "Complementarity and polarization modulation in photon interference," *Phys. Rev. Lett.* **119**(4), 040401 (2017).
12. A. Norrman, A. T. Friberg, and G. Leuchs, "Vector-light quantum complementarity and the degree of polarization," *Optica* **7**(2), 93–97 (2020).
13. X. Zhao, Y. Yao, Y. Sun, and C. Liu, "Condition for Gaussian Schell-model beam to maintain the state of polarization on the propagation in free space," *Opt. Express* **17**(20), 17888–17894 (2009).
14. M. Verma, P. Senthikumar, J. Joseph, and H. C. Kandpal, "Experimental study on modulation of Stokes parameters on propagation of a Gaussian Schell model beam in free space," *Opt. Express* **21**(13), 15432–15437 (2013).
15. Y. Gao, X. Li, Y. Cai, H. F. Schouten, and T. D. Visser, "Spectral polarization of Gaussian Schell-model beams," *Opt. Express* **28**(24), 35937–35945 (2020).
16. D. Kuebel and T. D. Visser, "Generalized Hanbury Brown–Twiss effect for Stokes parameters," *J. Opt. Soc. Am. A* **36**(3), 362–367 (2019).
17. L. Mandel and E. Wolf, *Optical Coherence and Quantum Optics* (Cambridge University Press, 1995).
18. T. Mukaihara, N. Ohnoki, Y. Hayashi, N. Hatori, F. Koyama, and K. Iga, "Excess intensity noise originated from polarization fluctuation in Vertical-Cavity Surface-Emitting Lasers," *IEEE Photonics Technol. Lett.* **7**(10), 1113–1115 (1995).
19. G. Wu, D. Kuebel, and T. D. Visser, "Generalized Hanbury Brown–Twiss effect in partially coherent electromagnetic beams," *Phys. Rev. A* **99**(3), 033846 (2019).
20. Y. Wang, S. Yan, D. Kuebel, and T. D. Visser, "Generalized Hanbury Brown–Twiss effect and Stokes scintillations in the focal plane of a lens," *Phys. Rev. A* **100**(2), 023821 (2019).
21. D. Goldstein, *Polarized Light*, 2nd ed. (Marcel Dekker, 2003) See Sec. 22.2.
22. M. Born and E. Wolf, *Principles of Optics*, 7th ed. (Cambridge University Press, 1995).
23. D. Kuebel and T. D. Visser, "Reconstruction of an electromagnetic Gaussian Schell-model source from far-zone intensity measurements," *Opt. Lett.* **45**(6), 1375–1378 (2020).
24. H. Zheng, W. Li, W. Li, X. Wang, Z. Tang, S. X. Zhang, and Y. Xu, "Uncovering the circular polarization potential of chiral photonic cellulose films for photonic applications," *Adv. Mater.* **30**(13), 1705948 (2018).
25. Z. Liu, C. Wu, Mi. V. Tse, C. Lu, and H. Tam, "Ultra-high birefringence index-guiding photonic crystal fiber and its application for pressure and temperature discrimination," *Opt. Lett.* **38**(9), 1385–1387 (2013).
26. R. M. A. Azzam, "Stokes-vector and Mueller-matrix polarimetry," *J. Opt. Soc. Am. A* **33**(7), 1396–1408 (2016).
27. F. Gori, M. Santarsiero, R. Borghi, and V. Ramírez-Sánchez, "Realizability condition for electromagnetic Schell-model sources," *J. Opt. Soc. Am. A* **25**(5), 1016–1021 (2008).